Influence of Lubricant Addition on Heat Exchange Regimes during Spray Cooling

Marija Gajevic Joksimovic*, Ilia V. Roisman, Cameron Tropea, Jeanette Hussong

Institute for Fluid Mechanics and Aerodynamics, Technical University Darmstadt, Darmstadt, Germany
*Corresponding author: gajevic-joksimovic@sla.tu-darmstadt.de

Keywords: Spray cooling, Lubricant solutions, Heat transfer regimes

ABSTRACT

Spray cooling is used in a variety of industries, including metallurgy, electronics, and medicine. Ease of spray generation, as well as the ability to cool relatively large surfaces or precise regions of interest, are among the key assets. Spray cooling can provide a relatively high heat flux, especially if it is accompanied by liquid evaporation. Additionally, it can be applied not only as a coolant but also as a transport medium for lubricating fluid in specific applications, such as hot die forging. Typically, the working fluid is a multi-component mixture with improved cooling and lubricating properties. Once the bulk liquid evaporates, particles or dissolved lubricant can settle on the hot solid substrate. Existence of components with various physico-chemical properties on the surface (binders, surfactants, dispersed particles, etc.) can significantly affect the spray impact, as well as the outcome of cooling regimes. Nevertheless, the accompanying thermal-hydraulic effects are still not well understood.

An experimental facility for observing the impact of the multi-component spray, and characterizing heat transfer was designed for this study at the Institute for Fluid Mechanics and Aerodynamics. As a working fluid, varied mixtures of water and industrial white lubricant were used in different ratios. The visualization of spray impact and identification of the main hydrodynamic regimes were achieved using a high-speed video system. The inverse heat conduction problem (Woodfield et al., 2006) was used to calculate the heat flux during continuous cooling from 445 °C to 100 °C, taking into account temperature readings from within the substrate. Since the substrate was entirely insulated on all sides (except on the sprayed surface), the boundary conditions were well defined. The experimental data for pure water drops were compared with the results obtained using lubricating additives. It is discovered that even minimal volumes of lubricant augment the heat flux dramatically, particularly at rather high wall temperatures. The spray cooling process is accompanied by an extensive foaming near the wall and as a result, the Leidenfrost point is moved to a higher temperature, thus suppressing film boiling regime.

1. Introduction

Spray impact onto a hot surface is often used in a variety of industrial applications. These applications include wall impact of a fuel spray in engines (Meingast et al., 2000; Lahane & Subramanian, 2014) or gas turbines, in selective catalytic reduction (SCR) systems of diesel driven

vehicles (A. Schmidt et al., 2021) as well as in other systems. Spray-induced cooling is extensively used during die forging, hot mill rolling (S.-J. Chen & Tseng, 1992), cooling of power electronics (H. Chen et al., 2022), etc. An extensive overview of spray cooling technology, with water or other one-component liquid being used as a working fluid, can be found in Kim (2007); Panão & Moreira (2009); W.-L. Cheng et al. (2016); Liang & Mudawar (2017a,b); Breitenbach et al. (2018) and elsewhere.

For moderate temperatures that do not exceed the saturation temperature, the cooling is realized mainly through the impact of single drops (Yarin et al., 2017), convection in a thin liquid wall film and through the evaporation at the free surfaces of the liquid layer. The cooling is enhanced significantly on structured substrates due to the local cooling in the neighborhood of the contact lines (Sodtke & Stephan, 2007; Z. Zhang et al., 2013; Xu et al., 2022).

At higher wall temperatures, the phenomena is accompanied by boiling and is influenced significantly by the corresponding thermodynamic phenomena. Different regimes have been observed during spray cooling at various wall temperatures and impact parameters. These regimes include nucleate boiling regime (Liang & Mudawar, 2017a; Breitenbach et al., 2017a), characterized by the heterogeneous nucleation of multiple bubbles on the wetted part of the solid surface; transition regime when the substrate surface is not uniformly wetted due to the percolation of the vapor in channels, formed by the coalescence of the bubbles (J. B. Schmidt et al., 2021); film boiling regime (Liang & Mudawar, 2017b; Breitenbach et al., 2017b; Castanet et al., 2018), characterized by the complete rebound of the impacting drops; and thermal atomization accompanied by the generation of an intensive flow of fine secondary drops (Roisman et al., 2018) in case of high impact velocities of the primary drops.

Recently, application of complex, multi-component liquids for the enhancement of spray cooling started to attract increased attention. Such liquids include suspensions, emulsions and solutions. In Singh & Kukreja (2021), an optimal concentration of the surfactant has been determined experimentally for sprays at temperature below the boiling point. It is known that at higher wall temperatures the addition of surfactants can significantly influence the phenomena of boiling and thus enhance spray cooling (Qiao & Chandra, 1998; W.-W. Zhang et al., 2018; Ravikumar et al., 2014; Liu et al., 2021). Moreover, the heat transfer can be influenced by the dissolution of different types of salts in the bulk liquid (Abdalrahman et al., 2014; W. Cheng et al., 2013; Pati et al., 2017). For example, Mohapatra et al. (2014) have noted that the heat flux at the surface of the very hot metal substrates at 900 °C, significantly increases by the addition of the dissolved salts in water used for cooling. Among the other fluids which can potentially enhance the spray cooling significantly are also nanofluids (Duursma et al., 2009; Sanches et al., 2021; Aksoy et al., 2020).

Behavior and properties of the liquid during spray cooling of hot substrates can change significantly due to the partial liquid evaporation. Correspondingly, the concentrations of the less volatile components grow. In some cases, this phenomenon leads to the deposition of additives at the wall surface. This process is used in some applications for applying surface coatings or lubrication. On the other hand, in other applications, such as in the engine fuel sprays, the fuel deposition is not a

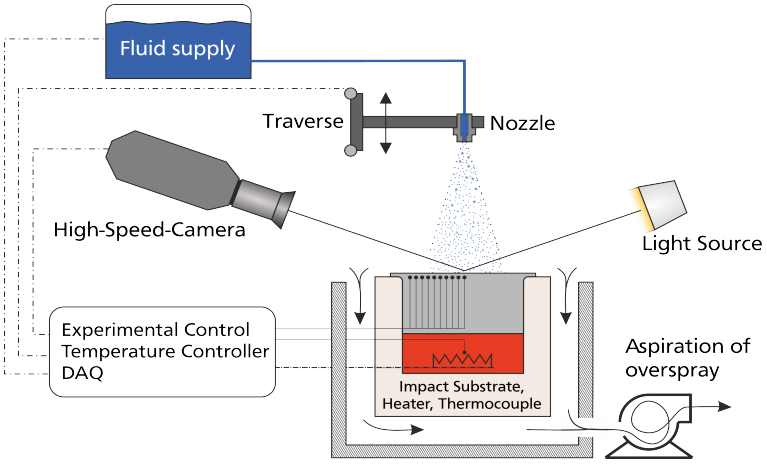

Figure 1. Schematic representation of the spray cooling experimental setup.

desirable process (Arters & Macduff, 2000).

The main influencing factors, affecting the behavior of multi-component liquids in a spray impacting a hot substrate still have to be identified. The main goal of this investigation is to observe, characterise and analyse the evolution of the heat flux during the spray cooling experiments, using an industrial water/lubricant mixture in different mixture ratios. Temperature and heat flux measurements are performed during continuous cooling of a thick metal target from 445 °C to 100 °C. These measurements are accompanied by high-speed visualizations of an impacting spray at various time instants, allowing identification of different spray cooling hydrodynamic and thermodynamic regimes, as well as the influence of different lubricant concentrations on the latter. It is found that the addition of even small amounts of lubricant increases the heat flux due to spray cooling significantly, especially at relatively high wall temperatures. Cooling time is therefore notably reduced in comparison to the pure water case. Moreover, spray cooling is accompanied by extensive foaming in the near wall region on substrates at high temperatures. Foaming phenomena are associated with a significant increase of the temperature of the Leidenfrost point and almost total suppression of the film boiling regime.

2. Experimental methodology

An experimental facility for observation and analysis of heat transfer due to spray impact onto a heated substrate has been built and is shown schematically in Fig. 1.

The configuration consists of six main systems, comprising a *spray generation system* connected to a fluid supply, *a heating system* with temperature measurement and control, *an observation system* with a high-speed camera with back light illumination and *computer control unit* for data acquisition and control of the experimental flow in *LabView* software.

The *spray generation system* is one of the most complex systems. For that reason, in Fig. 2, all of the components involved in the spray generating process are presented. The mixture of water with

industrial white lubricant in desired ratio is stored in a reservoir (1). If an elevated fluid temperature is needed, the immersion heater (2) connected to a temperature controller (3) is used. Mostly, in our experimental campaign, fluid remains at ambient temperature. The atomizer is driven by a gear pump (4) while corresponding fluid properties are measured by a pressure sensor (5) and a temperature sensor (6). A check valve separates the atomizer (9) from the main supply line (8). A directional valve connects the supply line to the recirculation line (7). Finally, a movable shutter (10) is situated right beneath the atomizer opening. This shutter can gather all of the spray that comes out of the atomizer for some amount of time, and serves for eliminating initial unsteadiness of the flow rate. It moves through the action of a pneumatic cylinder which instantly pushes the shutter into or out of the fluid stream. When the spray has reached a steady state, the shutter moves out of the flow and the spray can reach the hot substrate. This process prevents large fluid ligaments during atomizer unstable start-up phase, to reach the heated substrate.

After each spray experiment is completed, a solid residue is formed on the substrate. In order to start the next experiment, the substrate surface needs to be cleaned. For that purpose, a reservoir with a mixture of water and isopropanol is connected with mini-ball valves to a supply line (not presented in Fig. 2). During the cleaning, the mini-ball valves downstream of the fluid tank are closed in order to supply only the cleaning liquid to the whole system. The spray is produced by a water driven commercial nozzle (*Lechler 490.403*), a full-cone, pressure swirl and one component nozzle type. Different impact velocities of the spray droplets are achieved by varying the height of the spray above the hot substrate using a linear traverse. By adjusting the distance between the atomiser and the heated surface, and by varying the pressure supplied to the nozzle, sprays of different impact properties can be generated.

The atomizer has a bore diameter 1.25 mm, spray angle 45° and operating pressure from 1.5 to 10 bar. The upper limit of operational pressure is, however, dictated by the maximum differential pressure of the gear pump. The spray is characterized using phase Doppler measurements and the mass flow rates. The results of these measurements can be found in F. M. Tenzer (2020).

In order to measure a flow rate of the fluid passing through the atomizer, a Coriolis mass flow meter (*Optimass 7400 C* from *Krohne*) was installed.

The *heating system* consists of the spray impact target as a part of a watertight housing, including the heater. The heated target is the top end of a circular cylinder (diameter $d_t = 100$ mm and height $h_t = 53.2$ mm). The target is heated by four cartridge heaters *hotset hotrod HHP* with an overall power of 2 kW. All of the heaters are placed in a copper disc which is screwed to the bottom of the cylinder. The side and bottom of the target are insulated in order to assume that heat transfer only occurs through the top surface. The target is placed in a water resistant housing.

The material of the target is stainless steel with mirror polished upper surface made by lapping and polishing. The average roughness of the polished surface is < 0.03 μm. It was shown that stainless steel exhibits good resistance against corrosion and oxidation, thus, the spray target used in this experimental campaign endured more than 200 cooling experiments. The main challenge during

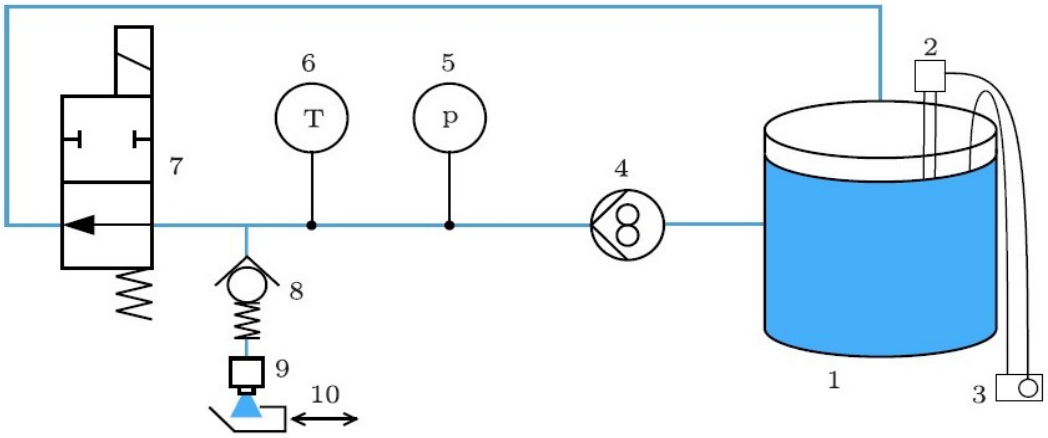

Figure 2. Detailed sketch of the atomizer and water supply system used for spray generation (F. M. Tenzer, 2020).

the construction of the heated target are achieving good thermal insulation and maintaining a watertight housing to ensure that a complete flooding of the target is possible without any damage to components. The setup is designed for surface temperatures up to 500 °C.

The observation system consists of a CMOS high-speed camera equipped with two different lenses and a back light illumination source. A camera is *Vision Research Phantom v2012* which can achieve a maximum resolution of 1280×800 pixels at 55000 fps, is used to record side-view images and videos of the spray impact. The high-speed camera is additionally equipped with a *Tamron* 180 mm macro optical lens. The back light illumination consists of a high powered light source (LED Illumination) and a diffusor plate. This illumination is placed behind the spray (and directed co-linear with the high-speed camera) resulting in shadowgraph imaging.

2.1. Measurement technique for heat flux and surface temperature

In order to evaluate both temperature and heat flux on the surface of the target, the inverse heat conduction problem (IHCP) needs to be solved by using the temperature readings from inside the substrate as input data. The boundary conditions can be determined from temperature data collected inside the domain by solving the IHCP. More specifically, by solving the IHCP, temperature and heat flux can be reconstructed at the surface of the substrate. The temperature readings are acquired from thermocouples embedded inside the target. In Fig. 3 the position of the thermocouples is shown. The thermocouples are type K, class 1, with 0.5 mm shield diameter. The measuring tip is open and aligned with the shield. This configuration ensures a fast response time. Thermocouples are arranged in two rows. The first row is located 0.5 mm below the surface to achieve a quick response time of all thermocouples. The holes, inside which the thermocouples are placed, are produced using the spark erosion technique. The resulting hole diameter is 0.6 mm. The thermocouples are bonded inside the holes using a thermally high conductive adhesive (*Aremco Ceramabond 569 VFG*) to ensure good thermal contact. Temperatures are sampled at a sample rate of 95 Hz using *National Instruments NI 9212* thermocouple input modules attached to a *National*

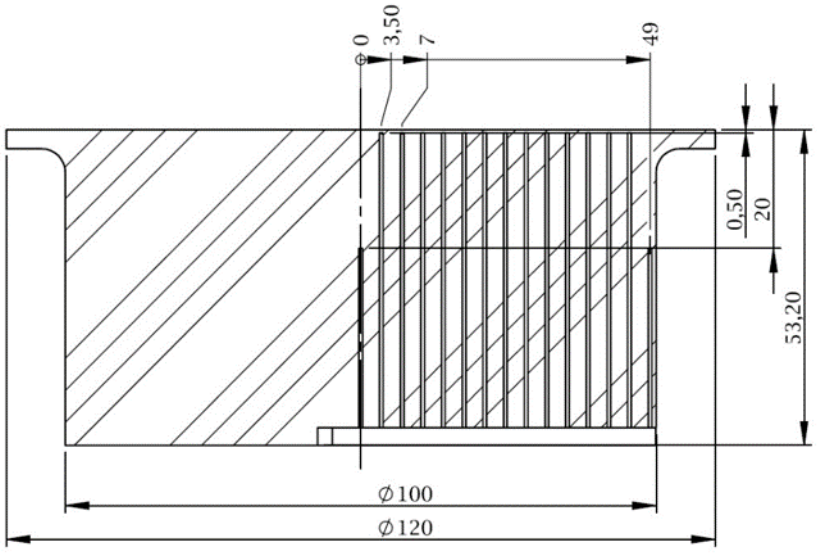

Figure 3. Sectional view of the heated target showing the thermocouple positions. Dimensions are in mm.

Instruments cRio 9074.

The radial distance between each sensor in the first row is 3.5 mm to account for any radial distribution of the heat flux. The second row is 20 mm below the surface to make the IHCP procedure independent of the boundary condition at the bottom of the target. Heat flux problem is assumed to be two-dimensional, axisymmetric and having adiabatic boundary conditions at the curved surface area.

The solution of IHCP is calculated by using a procedure published in Monde et al. (2003). Furthermore, Monde and coworkers developed and made an inverse heat conduction analysis code "Invers2D" available. In the present work, this tool is used for calculating the heat flux and surface temperature from temperature readings of the thermocouples. The procedure for applying the program is described in detail in Woodfield et al. (2006). Initially, the two-dimensional heat conduction problem is transformed from polar-cylindrical to the Laplace space. Time evolution of the measured temperature inside the target is approximated as a series of half power polynomials in time, and as Fourier-Bessel series in space. After solving the problem in Laplace space, an inverse Laplace transform leads to the solution.

2.2. Preparation of lubricant solutions

The industrial lubricant LUBRODAL F327,* produced by Fuchs LUBRITECH, is used as a base for the preparation of the solutions. The lubricant LUBRODAL F327 represents a water-miscible, graphite free, die lubricant with excellent separation effects for hot and warm forging of steel. It is widely used for different forging operations in industry because of quick formation of a well visible and touch-resistant lubrication film after spraying to the hot tool surfaces.

The lubricant is supplied as a concentrate, containing a specific amount of organic salts that provide lubrication when utilized. Organic and inorganic components (surfactants and binders) are present as well, in order to stabilize the concentrate and promote the spreading and formation of adherent lubricant layers on the die surface. However, the lubricant must be diluted with water to the desired ratio prior to use. After diluting, a further stirring of the working mixture is not necessary, because the main component, organic salt, is completely dissolved in water.

Solutions of different salt volume concentrations are prepared by mixing the concentrate with distilled water. In this study, the volumetric concentrations of the solutions range from $\varphi = 0.97\,\%$ to $\varphi = 5.47\,\%$. Experiments were conducted with 8 different lubricant-to-water mixture ratios, thus achieving different volumetric concentrations, as stated above. In most industrial applications, the maximum volumetric concentration of $\varphi = 8.2\,\%$ is typical as the upper limit, which is very rarely reached because of the spraying difficulties.

It is expected that lubricants will affect the heat flux by accelerating or suppressing various effects in nucleate boiling, transitional boiling, as well as in the film boiling regime during spray cooling. Since the concentration of the organic salts is small, it is expected that most of the thermal properties are similar to that of water. The boiling temperature of the mixture is $T_{\mathrm{sat}} = 100\ ^{\circ}\mathrm{C}$. The surface tension of the different solutions has been measured with a tensiometer. The surface tension of the solutions is respectively: $\sigma = 58.95$ mN/m for $\varphi = 5.47\,\%$, $\sigma = 61.63$ mN/m for $\varphi = 2.34\,\%$ and $\sigma = 64.28$ mN/m for $\varphi = 1.49\,\%$.

3. Results and discussions

Experiments in this study were performed with different lubricant-to-water mixture ratios (different organic salt volumetric concentrations), thus achieving various solution compositions. Additional experiments for the same spray and operational parameters were carried out with a pure water spray, for comparison purposes.

To evaluate the boiling curve in many heat transfer studies, setup configurations are usually designed to keep the substrate temperature constant. However, in our case, in order to evaluate effects of transient phenomena during spray cooling and in the same time lubrication, heated target temperature is kept constant only until the spray starts. First, the target is heated until a practically

*https://www.fuchs.com/lubritech/en/product/product/144158-lubrodal-f-327

uniform initial temperature of 445 °C is reached. Heating is stopped immediately after the start of spraying. Usage of a shutter in front of the nozzle removes the problem of the start-up phase during the initial development of the spray. Only once the spray has fully developed and the target has been uniformly heated, does the experiment begin.

Throughout the duration of the experiment, the spray parameters are kept constant, with the supply pressure of the atomizer at 2 bar. Visualization and heat flux measurements are temporally matched, and therefore visual observations can be directly associated with the instantaneous local heat flux and target surface temperature.

After each experiment (and complete liquid evaporation), solid residue remains on the substrate. In order to start a next experiment with a clean surface, cleaning liquid is pushed through the system. In this way, good repeatability between the experiments is achieved. The spray parameters for this case are: mass flow $\dot{m} = 62.1$ kg/h (dense spray), mean drop diameter $D_{10} = 78.7\,\mu$m and mean impact velocity $U = 14.05$ m/s.

3.1. Evolution of the heat flux and the wall temperature during spray cooling

The temporal evolution of the surface temperature and of the heat flux is shown in Fig. 4(a) and (b), respectively. The initial wall temperature is 450 °C. The experiments were stopped when the first thermocouple reading reached 100 °C.

The shape of the curves in Fig. 4(a), corresponding to different volume concentrations of the lubricant solutions, is similar. Leidenfrost point can be recognized as a kink in the corresponding curve indicating a sharp increase in the heat flux. Next, the critical heat flux (CHF) corresponds to the curve maximum. After reaching its maximum, the heat flux decreases monotonically.

Even a small amount of lubricant added to a spray liquid, as shown in Fig. 4, considerably changes the values of the heat flux, especially at the early stages of spray impact. The evolution of the heat flux and the substrate temperature is the same for distilled water and all lubricant solutions only during the first few seconds. As the lubricant concentration increases, the time instances corresponding to the Leidenfrost point and the CHF, as well as the total cooling duration, decrease significantly. In our experiments, the values of the Leidenfrost point increases from approximately 350 °C to 420 °C for the lubricant solutions of concentrations in the range from $\varphi = 0\,\%$ (distilled water) to $\varphi = 5.47\,\%$ (see Fig. 4b).

Interestingly, the Leidenfrost point seems to be nearly independent of the spray properties. Instead, it is strongly influenced by the material of the substrate and fluid: for a very high volumetric concentration ($\varphi = 5.47\,\%$), the film boiling phenomenon is almost totally suppressed even at a Leidenfrost point at a very high temperature, approximately 420 °C. With a decrease in volumetric concentration of lubricant solutions, the Leidenfrost point is accordingly moved to a lower temperatures. However, the duration of film boiling regime is still considerably smaller than that for distilled water case.

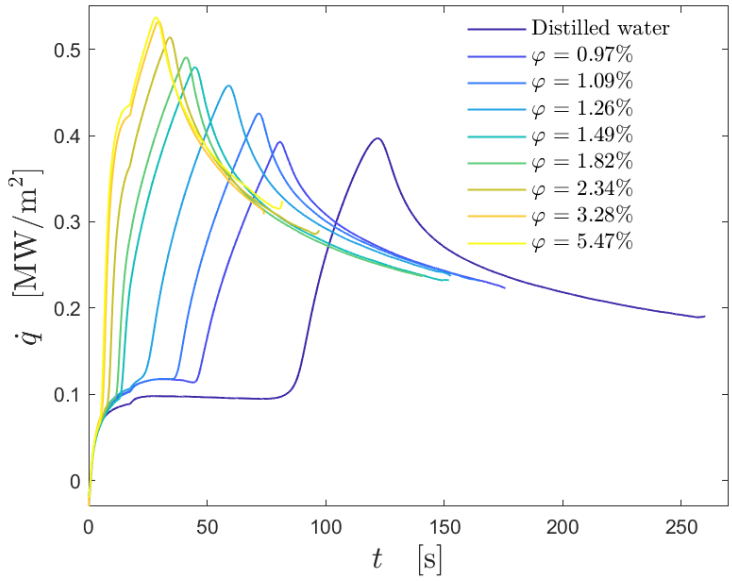

(a) Temporal evolution of the heat flux for different volume concentrations.

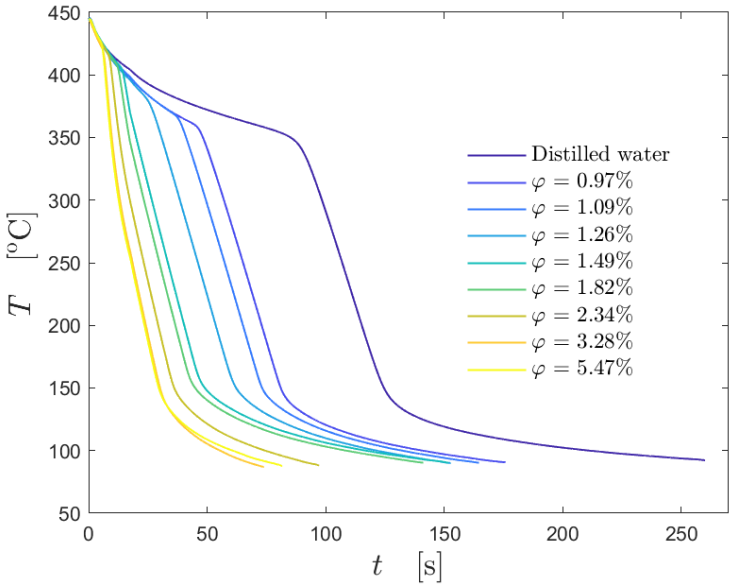

(b) Temperature evolution for different volume concentrations.

Figure 4. Boiling curves for spray cooling for different volume concentrations.

3.2. Phenomena of spray impact onto a hot substrate

Typical phenomena observed during spray cooling of a thick metal target by distilled water (F. Tenzer et al., 2019) are shown in Fig. 5, together with the corresponding boiling curve. The main phenomena include complete drop rebound in the film boiling regime, emergence of the wetted spots on the surface in the transition regime and formation of a fully developed liquid film at the substrate surface, accompanied by the nucleate boiling regime.

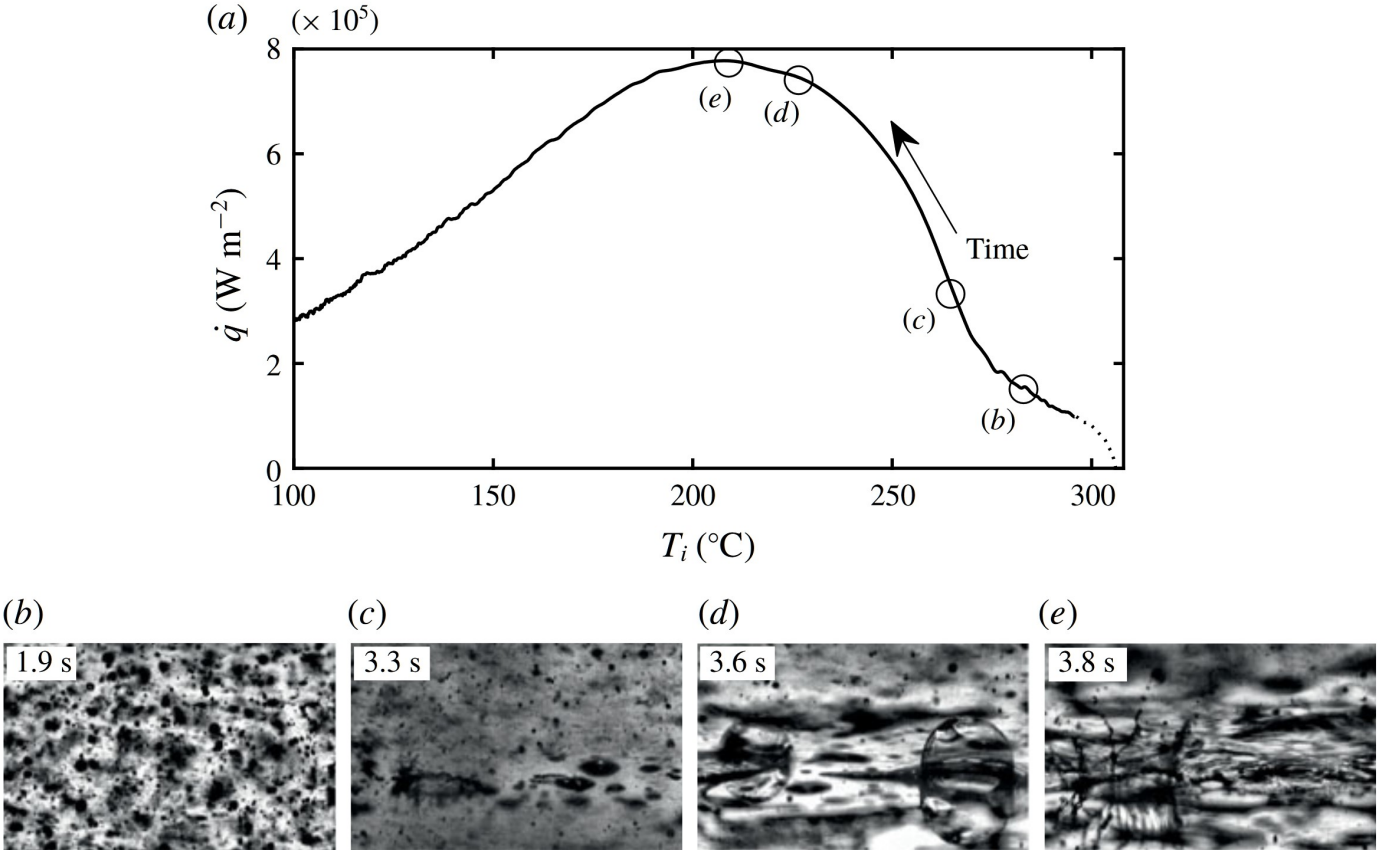

Figure 5. Observed regimes of distilled water spray at different surface temperatures $T(t)$. The boiling curve (a) and the images of the substrate during (b) film boiling regime; (c) inception of the transition regime; (d) fast expansion of the wetted area; (e) apparently completely wetted surface at the instant corresponding to the critical heat flux. This figure from F. Tenzer et al. (2019) is published with permission from Cambridge University Press.

When a slight amount of liquid lubricant is added to the liquid, the observed phenomena change significantly. An example is shown in Fig. 6. Separate wet spots form on the substrate surface within a short time after spraying begins. Next, liquid volumes generate a foam on a very hot substrate. The foam region expands until a full developed, relatively thick foam layer, is formed which coats the surface exposed to spray.

Now, evolution of the heat flux associated with spray cooling can be explained using a boiling curves for distilled water and for lubricant solution, shown exemplary in Fig. 7. Strong difference in the boiling curves of these two liquids is associated with the intensive liquid foaming of the

lubricant solutions.

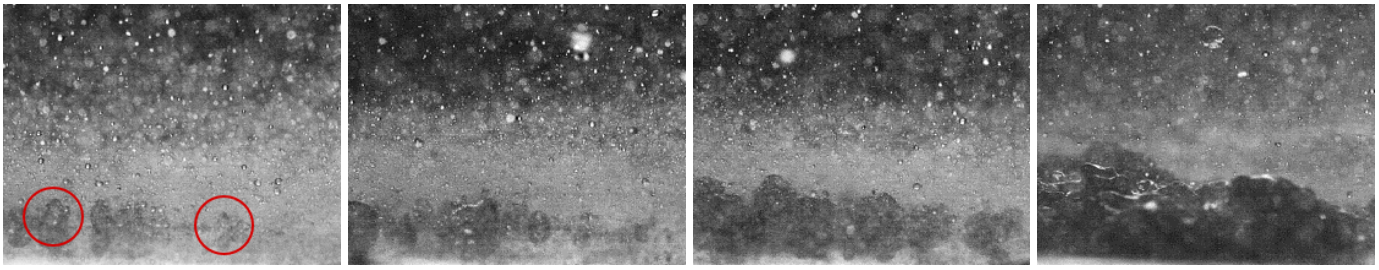

Figure 6. Impact of the $\varphi = 2.34\,\%$ solution. Shadowgraphy visualisations of a foaming phenomenon in 4 stages: from first appearance of foaming bubbles (denoted with red circles) to a completely developed foaming layer. Spray parameters correspond to the case shown in Fig. 7. Initial wall temperature was $T_{w0} = 445$ °C.

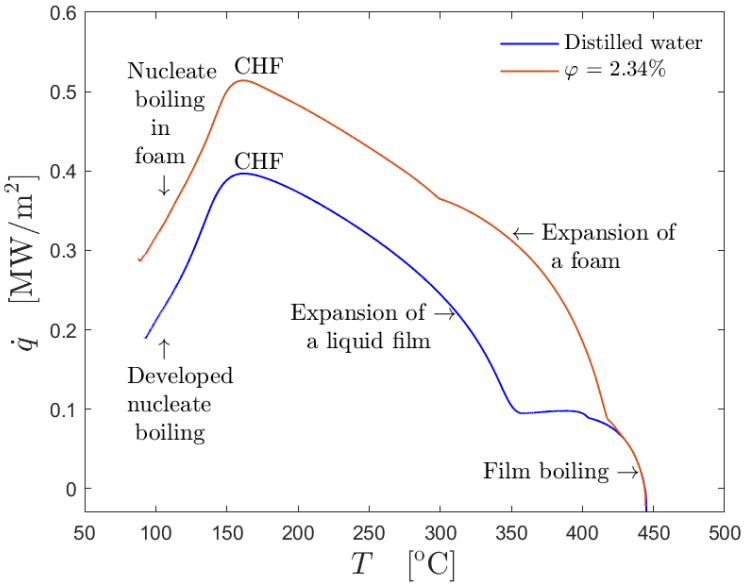

Figure 7. Boiling curves for distilled water in comparison with that for a lubricant solution $\varphi = 2.34\,\%$ for the same initial substrate temperature $T_{w0} = 445$ °C.

Evolution of a heat flux from the substrate temperature is shown in Fig. 7 for distilled water (blue line) as well as for a $\varphi = 2.34\,\%$ solution, for comparison purposes. The initial substrate temperature is $T_{w0} = 445$ °C.

In Fig. 8, the dependence of the boiling curves of a lubricant solution is shown for different initial wall temperatures. Even at lower substrate temperatures, far below Leidenfrost limit for water sprays, extensive foaming is observed. The observation results are shown in Fig. 9(a) and (b) for different initial wall temperatures.

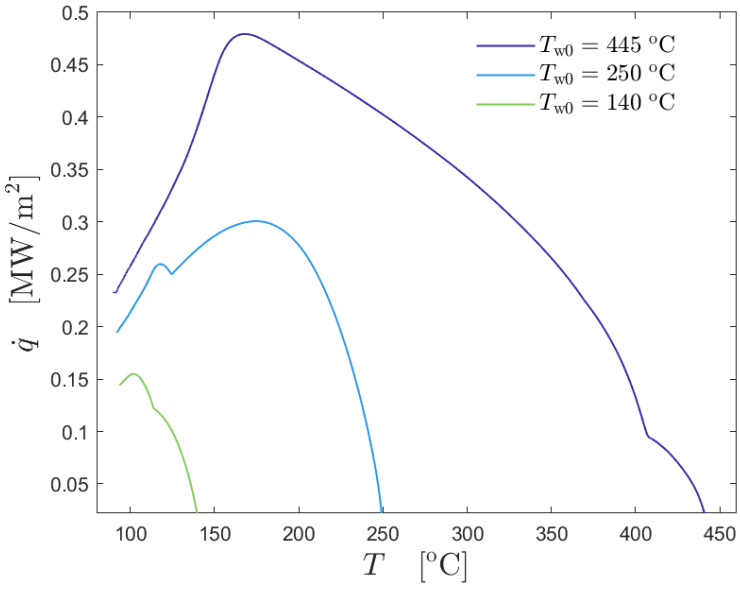

Figure 8. Comparison of the boiling curves of a lubricant solution $\varphi = 1.49\,\%$ for different initial substrate temperatures: $T_{w0} = 140$ °C, $T_{w0} = 250$ °C and $T_{w0} = 445$ °C.

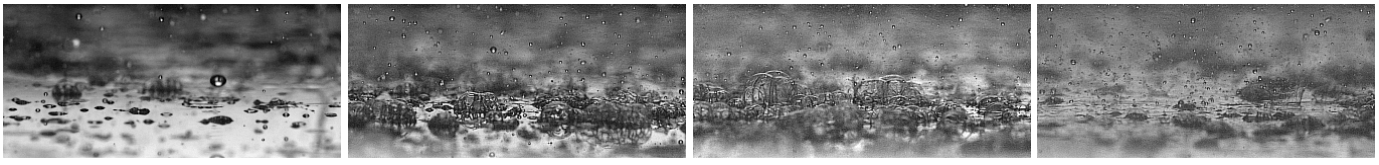

(a) $T_{w0} = 140$ °C

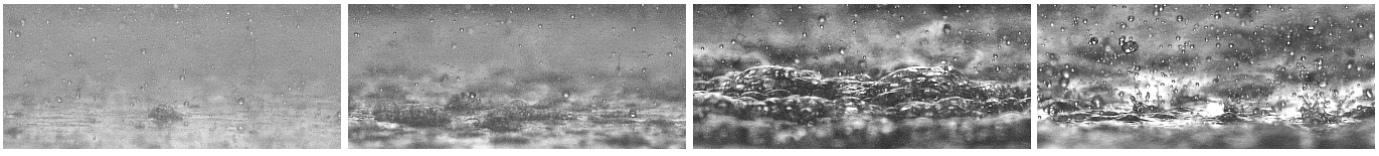

(b) $T_{w0} = 250$ °C

Figure 9. Observations of the phenomena accompanied with spray cooling using a lubricant solution $\varphi = 1.49\,\%$ for different initial wall temperatures, much below the Leidenfrost point for water.

3.3. Suppression of film boiling at high wall temperatures

At the wall temperatures well above the Leidenfrost point, rebound of distilled water drops is caused by the film boiling. Since the vapor layer between the liquid and the substrate serves as an insulation layer, the heat flux in this regime is relatively low. Even the small addition of lubricants changes the phenomena significantly. Intensive foaming prevents drop breakup and thus suppresses the film boiling phenomenon. Consequently, the measured heat flux is much higher than that for distilled water.

It is thus rather tempting to relate the foaming phenomena with the suppression of the film boiling.

However, this is not necessarily correct. Film boiling occurs mostly in a thin vapor layer with a thickness of a few hundreds of micrometers or less. The authors cannot find any physical reason for possible, significant influence of the foaming process on the transport processes associated with film boiling or even its suppression. In fact, the liquid foaming at very high temperatures and the suppression of the film boiling are caused by the same reason, identified as the presence of the salts and surfactants in lubricant solutions.

Namely, during a liquid drop impact onto a hot substrate, an intensive liquid vaporization occurs mainly in a close vicinity of the substrate surface. Certainly, a volatile liquid component, in our case water, evaporates first. The water evaporation leads to a fast local increase of the concentration of the salt and surfactant additives and even salt crystallization. The viscous layers of dense salt and surfactant solution cover expanding bubbles during water evaporation, thus leading to a formation of a stable foam. On the other hand, the salt and surfactant mixture deposit at the substrate surface forming a solid residue. This accreted wet granular layer leads to the pinning of the impacting drop, preventing drop rebound. The mechanism of the suppression of film boiling is analogous to the similar phenomena caused by the porous nano-fiber coatings (Weickgenannt et al., 2011). Such rough solid layers have been observed after spraying of hot substrates even for relatively dilute solutions of the lubricants.

4. Conclusions

In this study, the spray impact of different lubricant solutions onto a very hot substrate has been studied. The addition of a lubricant additive to a spray liquid does not lead to a significant change in the effective material properties of the spray liquid. Nevertheless, the presence of the dissolved organic salts from the lubricant influences significantly the heat transfer regimes during the spray cooling process.

We have discovered significant suppression of the film boiling regime, even for small volume concentrations, due to the appearance of the foaming phenomena near the wall region. Thus, cooling is accelerated, resulting in an increase of heat flux and consequently significantly shorter cooling times.

Furthermore, we have discovered that the presence of dissolved salts leads to significant changes in the well-known heat transfer regimes. At temperatures above the saturation temperature, instead of a nucleate boiling, foaming boiling is observed, where foaming bubbles do not detach from the substrate during boiling. Furthermore, the transitional phase is also followed by a foam appearance. Even at very high temperatures, much above the Leidenfrost point, the vapor layer is disturbed by the solid deposit formed from the dissolved salts and surfactants.

Acknowledgements

The authors gratefully acknowledge financial support from the Deutsche Forschungsgemeinschaft (DFG) in the framework of SFB-TRR 75 (TP T02, project number 84292822).

Nomenclature

t	Time [s]
d_t	Target diameter [mm]
h_t	Target height [mm]
φ	Volume concentration [%]
$\dot{m}$	Spray mass flow [kg/h]
σ	Surface tension [N/m]
D_{10}	Mean drop diameter [m]
U	Mean droplet velocity [m/s]
T_w0	Initial wall temperature [°C]
T	Surface temperature [°C]
$\dot{q}$	Local heat flux [W/m^2]

References

Abdalrahman, K. H. M., Sabariman, & Specht, E. (2014). Influence of salt mixture on the heat transfer during spray cooling of hot metals. *International Journal of Heat and Mass Transfer*, *78*, 76–83.

Aksoy, Y. T., Zhu, Y., Eneren, P., Koos, E., & Vetrano, M. R. (2020). The impact of nanofluids on droplet/spray cooling of a heated surface: A critical review. *Energies*, *14*(1), 80.

Arters, D. C., & Macduff, M. J. (2000). The effect on vehicle performance of injector deposits in a direct injection gasoline engine. *SAE Transactions*, 2044–2052.

Breitenbach, J., Roisman, I. V., & Tropea, C. (2017a). Drop collision with a hot, dry solid substrate: Heat transfer during nucleate boiling. *Physical Review Fluids*, *2*, 074301.

Breitenbach, J., Roisman, I. V., & Tropea, C. (2017b). Heat transfer in the film boiling regime: Single drop impact and spray cooling. *International Journal of Heat and Mass Transfer*, *110*, 34–42.

Breitenbach, J., Roisman, I. V., & Tropea, C. (2018). From drop impact physics to spray cooling models: a critical review. *Experiments in Fluids*, *59*, 1-21.

Castanet, G., Chaze, W., Caballina, O., Collignon, R., & Lemoine, F. (2018). Transient evolution of the heat transfer and the vapor film thickness at the drop impact in the regime of film boiling. *Physics of Fluids*, *30*(12), 122109.

Chen, H., Ruan, X.-h., Peng, Y.-h., Wang, Y.-l., & Yu, C.-k. (2022). Application status and prospect of spray cooling in electronics and energy conversion industries. *Sustainable Energy Technologies and Assessments*, *52*, 102181.

Chen, S.-J., & Tseng, A. A. (1992). Spray and jet cooling in steel rolling. *International Journal of Heat and Fluid Flow*, *13*(4), 358-369.

Cheng, W., Xie, B., Han, F., & Chen, H. (2013). An experimental investigation of heat transfer enhancement by addition of high-alcohol surfactant (HAS) and dissolving salt additive (DSA) in spray cooling. *Experimental Thermal and Fluid Science*, *45*, 198–202.

Cheng, W.-L., Zhang, W.-W., Chen, H., & Hu, L. (2016). Spray cooling and flash evaporation cooling: The current development and application. *Renewable and Sustainable Energy Reviews*, *55*, 614-628.

Duursma, G., Sefiane, K., & Kennedy, A. (2009). Experimental studies of nanofluid droplets in spray cooling. *Heat Transfer Engineering*, *30*(13), 1108–1120.

Kim, J. (2007). Spray cooling heat transfer: The state of the art. *International Journal of Heat and Fluid Flow*, *28*(4), 753–767.

Lahane, S., & Subramanian, K. (2014). Impact of nozzle holes configuration on fuel spray, wall impingement and nox emission of a diesel engine for biodiesel–diesel blend (b20). *Applied Thermal Engineering*, *64*(1-2), 307–314.

Liang, G., & Mudawar, I. (2017a). Review of spray cooling – part 1: Single-phase and nucleate boiling regimes, and critical heat flux. *International Journal of Heat and Mass Transfer*, *115*, 1174-1205.

Liang, G., & Mudawar, I. (2017b). Review of spray cooling – part 2: High temperature boiling regimes and quenching applications. *International Journal of Heat and Mass Transfer*, *115*, 1206-1222.

Liu, P., Kandasamy, R., Ho, J. Y., Feng, H., & Wong, T. N. (2021). Comparative study on the enhancement of spray cooling heat transfer using conventional and bio-surfactants. *Applied Thermal Engineering*, *194*, 117047.

Meingast, U., Staudt, M., Reichelt, L., Renz, U., & Sommerhoff, F.-A. (2000). Analysis of spray/wall interaction under diesel engine conditions. *SAE transactions*, 299–312.

Mohapatra, S. S., Ravikumar, S. V., Jha, J. M., Singh, A. K., Bhattacharya, C., Pal, S. K., & Chakraborty, S. (2014). Ultra fast cooling of hot steel plate by air atomized spray with salt solution. *Heat and Mass Transfer*, *50*(5), 587–601.

Monde, M., Arima, H., Liu, W., Mitutake, Y., & Hammad, J. (2003, 06). An analytical solution for two-dimensional inverse heat conduction problems using Laplace transform. *International Journal of Heat and Mass Transfer*, *46*, 2135-2148.

Panão, M. R., & Moreira, A. L. (2009). Intermittent spray cooling: a new technology for controlling surface temperature. *International Journal of Heat and Fluid Flow*, *30*(1), 117–130.

Pati, A. R., Behera, A., Munshi, B., & Mohapatra, S. S. (2017). Enhancement of heat removal rate of high mass flux spray cooling by sea water. *Experimental Thermal and Fluid Science*, *89*, 19–40.

Qiao, Y. M., & Chandra, S. (1998, 02). Spray cooling enhancement by addition of a surfactant. *Journal of Heat Transfer*, *120*(1), 92-98.

Ravikumar, S. V., Jha, J. M., Sarkar, I., Pal, S. K., & Chakraborty, S. (2014). Enhancement of heat transfer rate in air-atomized spray cooling of a hot steel plate by using an aqueous solution of non-ionic surfactant and ethanol. *Applied thermal engineering*, *64*(1-2), 64–75.

Roisman, I. V., Breitenbach, J., & Tropea, C. (2018). Thermal atomisation of a liquid drop after impact onto a hot substrate. *Journal of Fluid Mechanics*, *842*, 87–101.

Sanches, M., Marseglia, G., Ribeiro, A. P., Moreira, A. L., & Moita, A. S. (2021). Nanofluids characterization for spray cooling applications. *Symmetry*, *13*(5), 788.

Schmidt, A., Bonarens, M., Roisman, I. V., Nishad, K., Sadiki, A., Dreizler, A., ... Wagner, S. (2021). Experimental investigation of adblue film formation in a generic scr test bench and numerical analysis using les. *Applied Sciences*, *11*(15), 6907.

Schmidt, J. B., Hofmann, J., Tenzer, F. M., Breitenbach, J., Tropea, C., & Roisman, I. V. (2021). Thermosuperrepellency of a hot substrate caused by vapour percolation. *Communications Physics*, *4*(1), 1–8.

Singh, S., & Kukreja, R. (2021). Experimental study on effects of surfactant and spray inclination on heat transfer performance in nonboiling regime. *Energy Sources, Part A: Recovery, Utilization, and Environmental Effects*, 1–15.

Sodtke, C., & Stephan, P. (2007). Spray cooling on micro structured surfaces. *International Journal of Heat and Mass Transfer*, *50*(19-20), 4089–4097.

Tenzer, F., Roisman, I. V., & Tropea, C. (2019, 12). Fast transient spray cooling of a hot thick target. *Journal of Fluid Mechanics*, *881*, 84-103.

Tenzer, F. M. (2020). *Heat transfer during transient spray cooling: An experimental and analytical study* (PhD thesis). Technische Universität Darmstadt, Darmstadt, Germany.

Weickgenannt, C. M., Zhang, Y., Sinha-Ray, S., Roisman, I. V., Gambaryan-Roisman, T., Tropea, C., & Yarin, A. L. (2011). Inverse-leidenfrost phenomenon on nanofiber mats on hot surfaces. *Physical Review E*, *84*(3), 036310.

Woodfield, P., Monde, M., & Mitsutake, Y. (2006, 08). Improved analytical solution for inverse heat conduction problems on thermally thick and semi-infinite solids. *International Journal of Heat and Mass Transfer*, *49*, 2864-2876.

Xu, R., Wang, G., & Jiang, P. (2022). Spray cooling on enhanced surfaces: A review of the progress and mechanisms. *Journal of Electronic Packaging*, *144*(1).

Yarin, A. L., Roisman, I. V., & Tropea, C. (2017). *Collision phenomena in liquids and solids*. Cambridge, UK: Cambridge University Press.

Zhang, W.-W., Li, Y.-Y., Long, W.-J., & Cheng, W.-L. (2018). Enhancement mechanism of high alcohol surfactant on spray cooling: Experimental study. *International Journal of Heat and Mass Transfer*, *126*, 363–376.

Zhang, Z., Li, J., & Jiang, P.-X. (2013). Experimental investigation of spray cooling on flat and enhanced surfaces. *Applied Thermal Engineering*, *51*(1-2), 102–111.